Machine Learning and Experimental Study on the Fe_2O_3 Nanoparticles Blended Waste Cooking Oil Biodiesel on the Performance Of CI Engine

Manav Khera[1*], Abhendra Pratap Singh[2], Md Ehsan Asgar[3], Uma Gautam[4], Rajeev Ranjan[5], and Nandini Sharma[6]

[12,3,4,5]Department of Mechanical Engineering, HMRITM, Hamidpur, New Delhi., 110036, India
[6]Department of Computer Science and Engineering, HMRITM, Hamidpur, New Delhi., 110036, India
[*]mkhera2004@gmail.com

* Corresponding author

doi: https://doi.org/10.21467/proceedings.7.6.32

Abstract

The conventional fuels, being non-renewable and having adverse implications on environment, are not viable to be in use for much longer. This leads to the growing demand of a potential alternative which is both accessible and cleaner. The biofuel is one such promising solution aimed to reduce the reliance on fossil fuels while contributing to cleaner combustion. However, when used directly in engines, biofuels lead to incomplete combustion and escalated rate of exhaust emissions. This study hence aims to introduce and experimentally analyse the biofuels to overcome these limitations. As cooking oil is considered as waste and discarded after been used a few times, this cooking oil is being analysed with or without the addition of nanoparticles to perform a comparative experiment to reach the most suitable solution among them. This experimental research focuses on the utilization of metal oxide nano particles enhanced biofuels, optimizing the emission aspect and efficiency of fuel. A blend of 10% biofuel, both in presence and absence of, 50ppm iron oxide nano fuel, another blend of 15% biofuel with or without 50ppm iron oxide nanoparticles and pure diesel have been analysed in a variable CI engine. These samples are tested experimentally for various fuel characteristics such as fuel properties, BTE, viscosity and pollutant emissions reduction. Additionally, machine learning models, linear regression and random forest regression, are further used to calculate the biodiesel production process's response traits in regard to the process parameters. Hence, this study aims to examine the effect nano particles exhibit on fuel properties, combustion performance, and emission aspect. This could further contribute to the development of cleaner and more effective biofuels.

Keywords: brake thermal efficiency, biodiesel, nanoparticles blends, machine learning

1. Introduction

Conventional fuels like petroleum, coal and natural gas, called as fossil fuels, have contributed to provide energy majorly worldwide for decades. Fossil fuels being a non-renewable resource, are hence expected to deplete soon as a result of escalating demand due to rapid population growth and industrialization. Additionally, utilization of fossil fuels has contributed in harmful state of the environment. The usage of these resources led to the exhibition of pollutants which are considered harmful for the environment. This leads to the requirement of cleaner, cost efficient and easily accessible renewable energy resource. One such resource is biofuels which are energy infused chemicals produced by the biological mechanisms [1]. They can be used as a potential alternative for these fuels due to its similarity in properties of PBD fuel. Biofuels however is a generic term used for any liquid source derived from renewable sources. Under this falls a more specific field known as biodiesel. Biodiesel is obtained through process of transesterification of oils or fats, taken from biological organisms [2]. It is recognized as being non-toxic, non-flammable and sustainable, generating fewer substance outflow which are harmful to ozone and security of supply [3].

Biofuels have a promising potential to be the alternative to fossil fuels due to its many advantages. These fuels are biodegradable, renewable and can noticeably reduce greenhouse gas emissions. The second generation biofuels, especially those which lack lignocellulosic biomass, have been observed to emit substantially less greenhouse gases than conventional fossil fuels [4]. Moreover, it is possible to produce biofuels locally by using regionally available biomass resources. Thus, this local production aids in stimulating economies by producing employment opportunities in agriculture, manufacturing, and transportation sectors as well as reducing reliance on imported petroleum which further enhances energy security [5]. Accessibility and cost effectiveness plays a major role in widespread adoption of biofuels. while fossil fuels require complex extraction and refining processes, Biofuels can be synthesized from various waste materials. This makes the biofuels more effective for regions having limited fossil fuels reserves. The production of these fuels is simple and a wide range of feedstocks like plant oils, waste materials are available. This leads to biofuels being more inclusive and scalable energy solution. This

Proceedings DOI: 10.21467/proceedings.7.6; Series: AIJR Proceedings; ISSN: 2582-3922; ISBN: 978-81-989164-9-5

accessibility ensures a consistent supply with recycling of waste products and aids circular economy models through the conversion of waste into valuable fuel [6].

In India, the waste cooking oil is considerably large, with significant quantities often thrown away improperly or reused unsafely, proving to be fatal to environment as well as health. Utilizing this oil as a feeding stock to produce biodiesel presents a viable solution to waste management issues while contributing to renewable energy generation. It was seen that biodiesel obtained from this oil gives out fuel properties comparable to those of petroleum diesel, making it a dependable alternative fuel source [7]. In order to improve the efficiency and emission aspect of biodiesel, recent research has explored the combining nanoparticles with this fuel. Incorporating metal based nanoparticles such as iron oxide (Fe_3O_4) into biodiesel blends has been shown to improve combustion efficiency, increase brake thermal efficiency, and reduce harmful emissions [8]. The catalytic effect of these nanoparticles improves the fuel–air mixture quality, resulting in more complete combustion [9].

This study explores the discarded cooking oil's potential to replace the existing fuels as biodiesel, with iron oxide nanoparticles added to enhance the fuel properties. This research aims to investigate improvements in key parameters of the biofuel with or without the nanoparticles. Moreover, response traits of the biodiesel production process with respect to the parameters of the process are estimated using machine learning models such as linear regression and random forest regression. This study is further conducted to analyse the feasibility of this nanoparticle enhanced blend biodiesel as a sustainable and efficient solution to replace conventional fuels.

2. Materials and Methods

2.1 Nanoparticles Synthesis

Co-precipitation is the primarily used procedure to obtain iron oxide nanoparticles. The process consists of combining molar ratio 1:2 of ferric and ferrous ions in extremely alkaline medium at either ambient or elevated temperature as shown in Fig 1. The magnetic particles are obtained most likely by this method due to its high efficiency. Also, Sudeshkumar et al. observed the reliability and scalability in producing nanoparticle additives through the process of co-precipitation in fuel blend research [10]. Generally, iron oxide nanoparticles are prepared through an aging stoichiometric mixture of ferrous with ferric salts in aqueous solution as depicted in Fig 2 and 3.

Fig.1. Coprecipitation Process

Fig.2. Iron Oxide Nanoparticles Process

Fig.3. Nanoparticles of Iron Oxide

Proceedings DOI: 10.21467/proceedings.7.6
ISBN: 978-81-989164-9-5

Series: AIJR Proceedings
ISSN: 2582-3922

2.2 Production of Biodiesel

The waste mustard oil is undergone transesterification process to obtain biodiesel. The single stage transesterification process is applied to obtain biodiesel for this study as illustrated in Fig 4 and Fig5. It is seen that utilization of alkali catalysts in single-stage transesterification leads to improved quality of biodiesel when the feedstock has less free fatty acids [11]. Additionally waste mustard oil is easily accessible from restaurants, vendors and sweet shops. This biodiesel production was conducted using substances such as potassium hydroxide (KOH), methanol shown in Fig 6 and Fig 7.

Fig4. Filtration of Biodiesel

Fig5. Biodiesel

Fig6. Methanol

Fig7. KOH

2.3 Nanoparticles blending with biodiesel

The iron oxide nanoparticles were used to analyse their impacts on the diesel biodiesel blend. The ultrasonication, given in Fig8, is widely used to disperse nanoparticles uniformly in liquid fuels which effectively reduces the chances of agglomeration and also improves stability[12]. Likewise, mechanical agitation helps in the even distribution of nanoparticles, which promotes homogeneity of the blend formed [13]. The preparation of nanoparticle blended biodiesel includes the steps as explained in the next section.

Fig.8. Ultrasonication process

2.4 Prediction of Biodiesel Properties using Machine Learning

Linear Regression. The dependent variable (y) is predicted via linear regression, which expresses it as a linear function of the predictor variable (x). Regression problems with a single predictor variable typically have a monotonic relationship between y and x, meaning that any change in x will cause y to rise or decrease. A best line fit of the following type is then performed on the general trend revealed by a scatter plot between x and y. as shown in equation (1) and Fig.9

$$y = a + bx \quad (1)$$

Proceedings DOI: 10.21467/proceedings.7.6
ISBN: 978-81-989164-9-5

Series: AIJR Proceedings
ISSN: 2582-3922

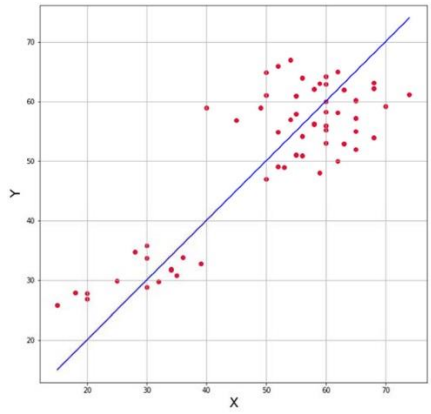

Fig.9. Biodiesel properties prediction of Linear Regression model [14]

Random Forest. Based on the ideas of bagging and random subspace approaches, random forest regression is an ensemble methodology. An ensemble of learner trees is produced by bootstrap aggregation or bagging. Independent and distinct bootstrap samples taken from the first training dataset are used to train these learner trees. A bootstrap sample (Db) is created by randomly selecting n examples from an original training dataset, D, with replacement, out of D's N examples. With no duplicate instances, Db is around two-thirds of D. For the bootstrap samples, K separate regression trees are constructed using input vector x as shown in equation (2) and Figure 10. In general, these regression trees exhibit high variance and low bias.

$$\text{Random forest prediction} = \frac{1}{K}\sum_{K=1}^{K} h_K(x) \qquad (2)$$

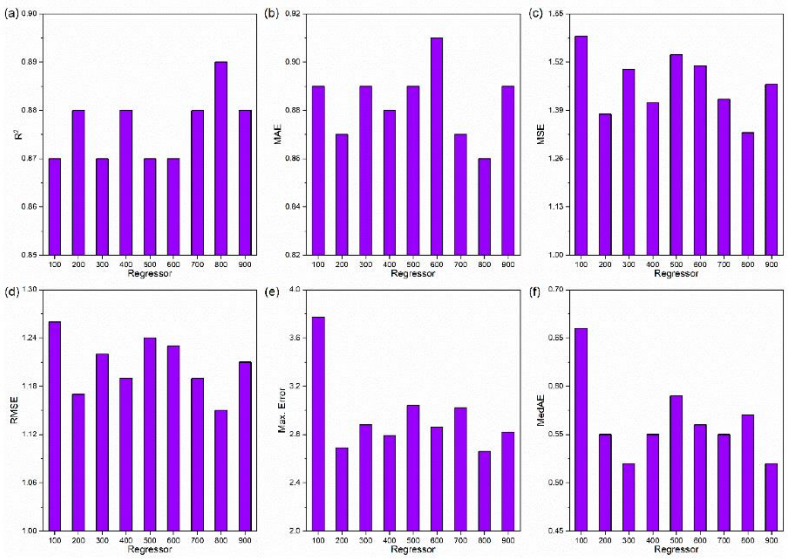

Fig.10. Biodiesel properties prediction of Random Forest Regression model [15]

3. Experimental set-up

4 Stroke CI Engine. The experiment set up used in our process was variable compression ratio ignition engine in which the load and other parameters are varied. In this set up various blends of biodiesel are used and nanoparticles in these blends are added in order to enhance the efficacy of the engine. The below Figure 11 represents the single cylinder 4 strokes, variable CI engine.

Proceedings DOI: 10.21467/proceedings.7.6
ISBN: 978-81-989164-9-5

Series: AIJR Proceedings
ISSN: 2582-3922

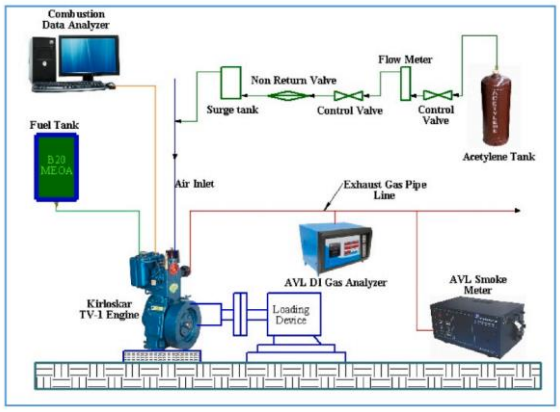

Fig.11. Single cylinder four strokes, variable CI engine [16]

Pensky Martin. The minimum temperature, at which a distinct flash can be seen when flame of sample introduced into the cup of oil, is referred to as the flash point [17]. The temp at which the sample begins to burn consistently for at least 5seconds, is referred to as the fire point. The oil sample is collected in the oil cup. The sample is measured using a point marked on this cup.

4. Results and Discussions

4.1 Fuel properties

υ , Kinematic Viscosity. The υ values for various blends of biodiesel, both in presence and absence of Fe_2O_3, are illustrated in Fig12.

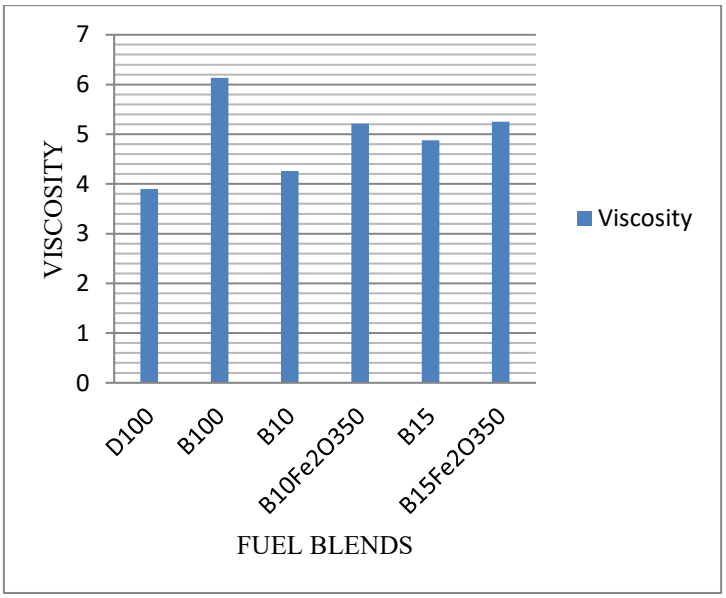

Fig.12. υ variation of biodiesel blends

A further increment was observed in the kinematic viscosity for the biodiesel blend when immersed 50ppm amount of nanoparticles. The $B_{15}Fe_2O_350$ blend obtained the maximum kinematic viscosity.

Flash Point (FP). The FP values for various blends of biodiesel, both in presence and absence of iron oxide nanoparticles, are illustrated in Fig13.

Proceedings DOI: 10.21467/proceedings.7.6
ISBN: 978-81-989164-9-5

Series: AIJR Proceedings
ISSN: 2582-3922

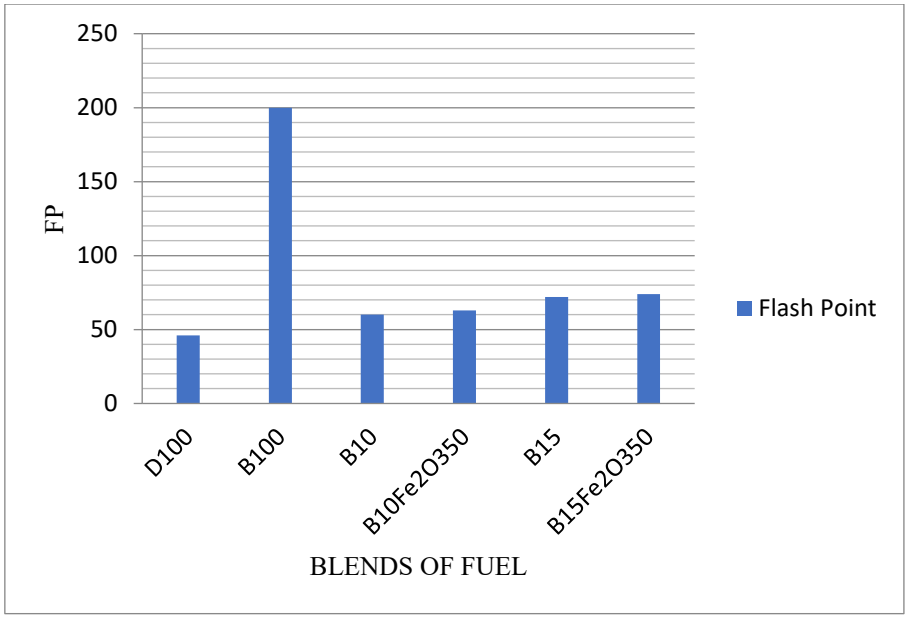

Fig 13. Flash point variation

A further increment was observed in the flash point of biodiesel blend with inclusion of nanoparticles. The decrement of volatility of nanoparticles added fuel resulted in the increase of flash point.

4.2 Performance Characteristics

Brake power (BP).

Effect of blend and load on brake power . The Fig 14, 15 and 16 illustrates the variation of BP with load of various blends at CR 14, 16 and 18 respectively. At full load and all CR, results are mentioned in Table 1.

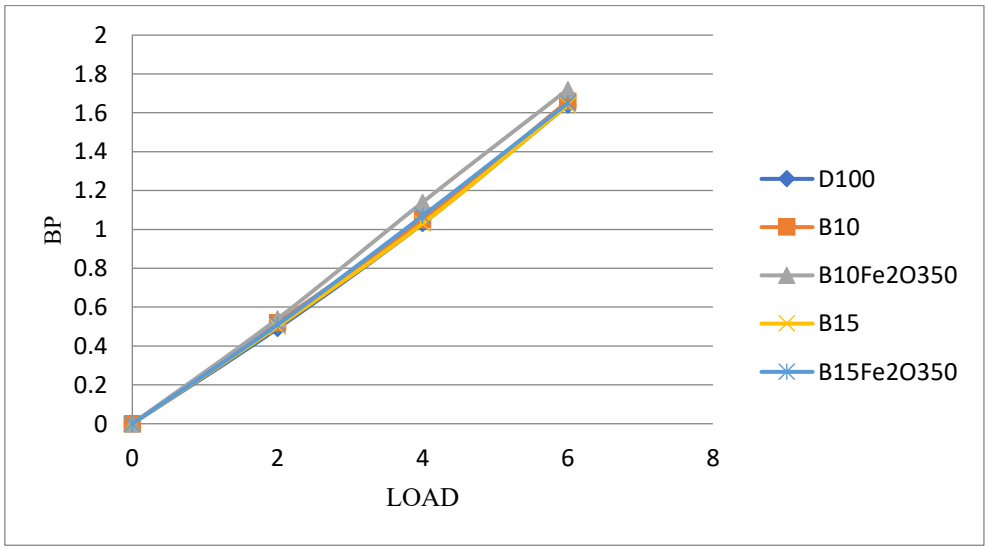

Fig.14. Brake power variation at CR 14

Proceedings DOI: 10.21467/proceedings.7.6
ISBN: 978-81-989164-9-5

Series: AIJR Proceedings
ISSN: 2582-3922

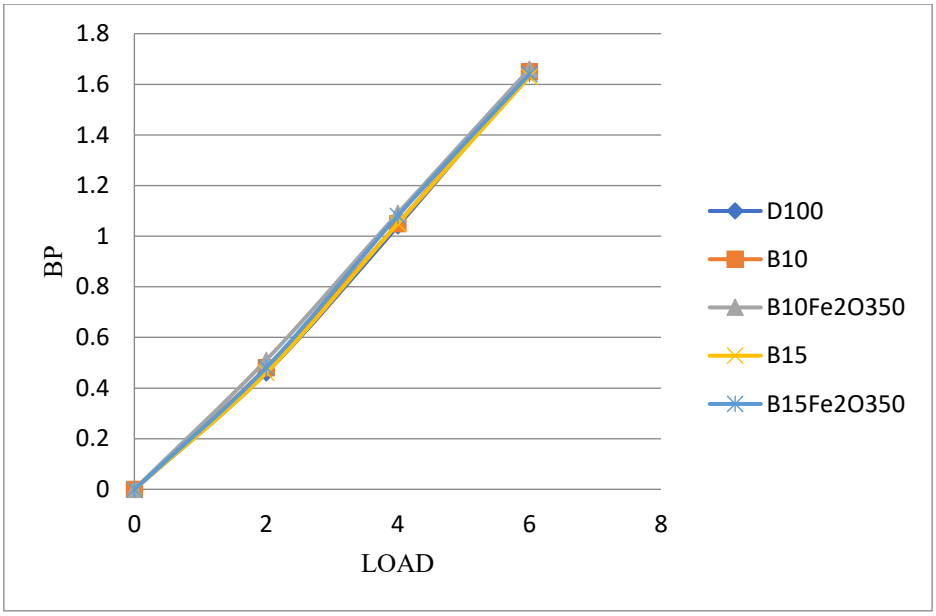

Fig.15. BP variation at CR 16

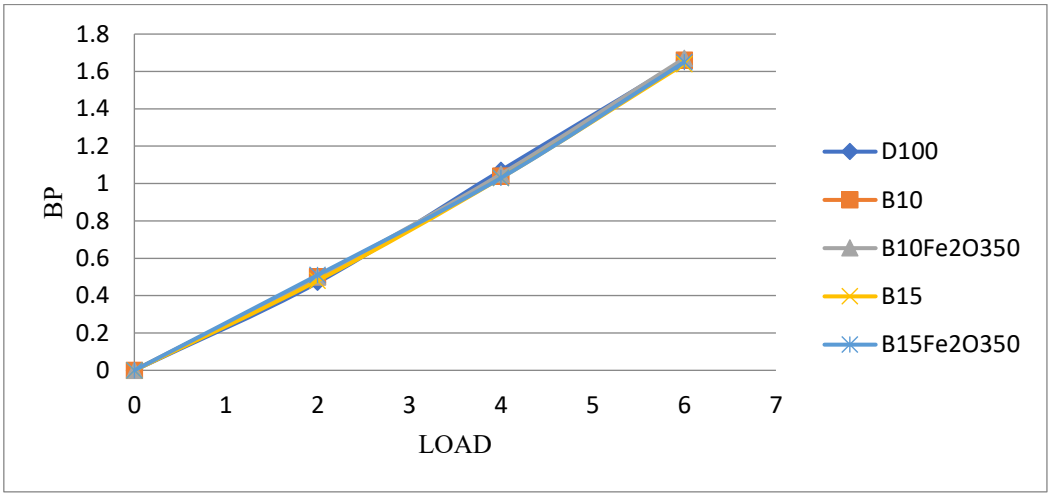

Fig.16. BP variation at CR 18

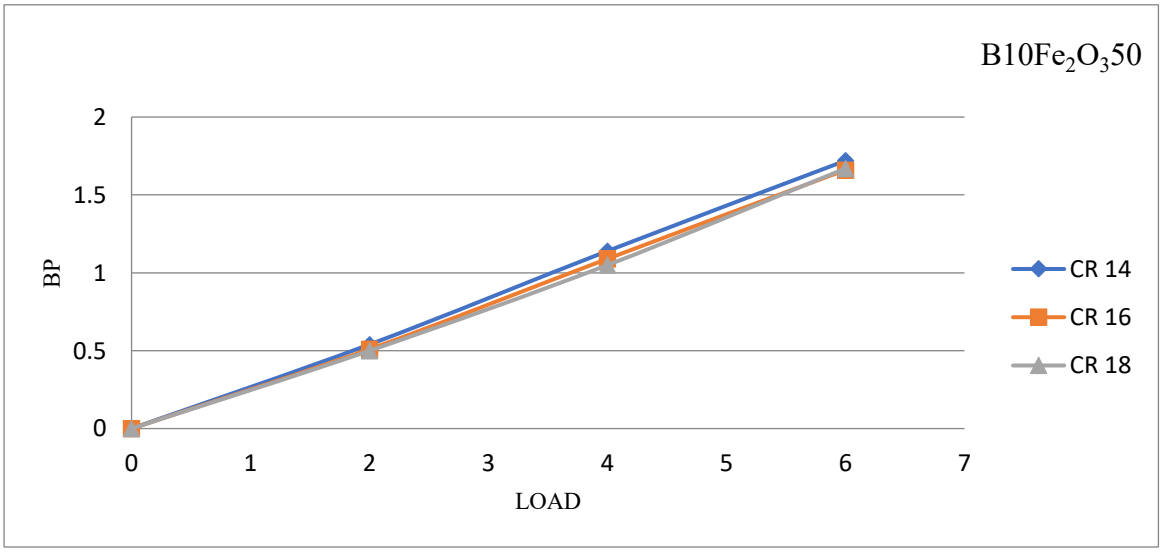

Fig.17. BP variation of B10$Fe_2O_3$50 at CR 14, 16 and 18

Proceedings DOI: 10.21467/proceedings.7.6
ISBN: 978-81-989164-9-5

Series: AIJR Proceedings
ISSN: 2582-3922

Effect of compression ratio on BP. The Fig 17 illustrates the variation of BP at CR 14, 16, and 18 according to the load for optimized blend of biodiesel B 10 Fe_2O_3 50. At full load and CR 14, the biodiesel blend B 10 Fe_2O_3 50 was seen to generate maximum power due to mechanical energy being fully converted from chemical energy as shown in Table 1.

Table 1. Brake power with full load condition

BP (kW) for full load conditions			
Compression Ratio	14	16	18
D 100	0.54	0.55	0.56
B 10	0.56	0.55	0.56
B10 Fe_2O_3 50	0.62	0.56	0.57
B 15	0.54	0.53	0.54
B 15 Fe_2O_3 50	0.55	0.54	0.55

Brake thermal efficiency (BTE).

Impact of blend and load on BTE. At different load and CR 14, 16 and 18, the tests were performed for the diesel taken as base fuel and various blends of biodiesel samples taken B 10, B 10 Fe_2O_3 50, B 15, and B 15 Fe_2O_3 50 as illustrated in Fig 18, 19, and 20. The Table 2 showcases all the results obtained for all the fuels at all CRs and full load.

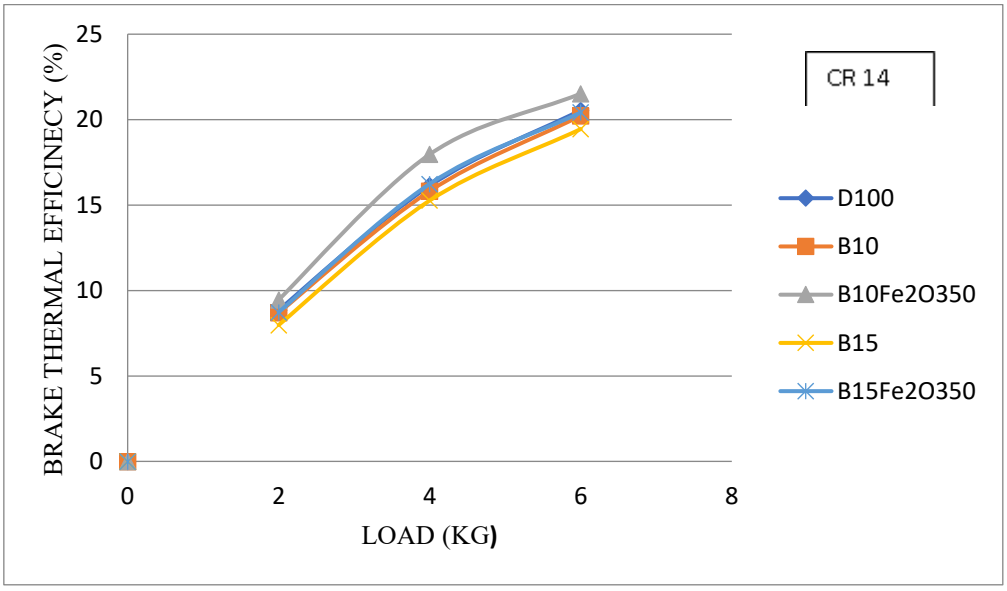

Fig.18. BTE variation at CR 14

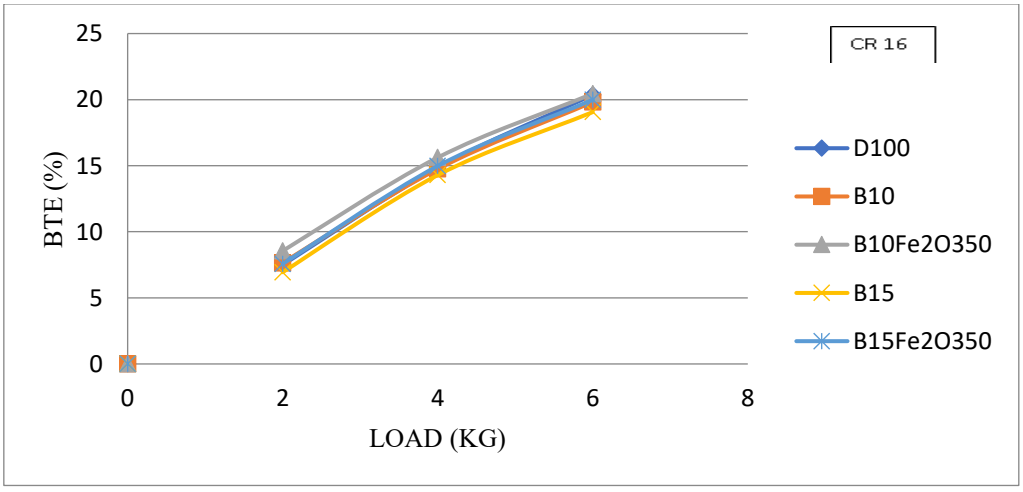

Fig.19. BTE variation at CR 16

Proceedings DOI: 10.21467/proceedings.7.6
ISBN: 978-81-989164-9-5

Series: AIJR Proceedings
ISSN: 2582-3922

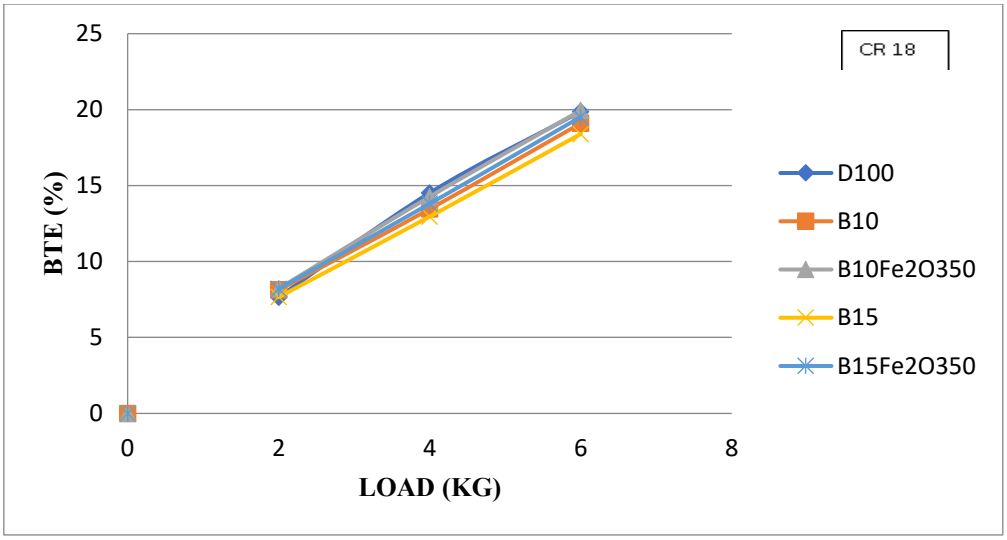

Fig.20. BTE variation at CR 18

Table 2. BTE for all fuels with CRs (%)

CR	LOAD	D 100	B 10	B 10 Fe_2O_3 50	B 15	B 15 Fe_2O_3 50
14	0	0	0	0	0	0
	2	7.85	7.69	8.45	6.97	7.72
	4	16.13	15.82	17.97	15.27	16.24
	6	20.55	20.23	21.52	19.45	20.42
16	0	0	0	0	0	0
	2	7.49	7.65	8.55	6.94	7.57
	4	14.85	14.75	15.62	14.29	14.98
	6	20.36	19.82	20.45	19.06	19.99
18	0	0	0	0	0	0
	2	7.65	8.12	8.21	7.66	8.2
	4	14.52	13.46	14.27	12.96	13.81
	6	19.87	19.1	19.95	18.4	19.52

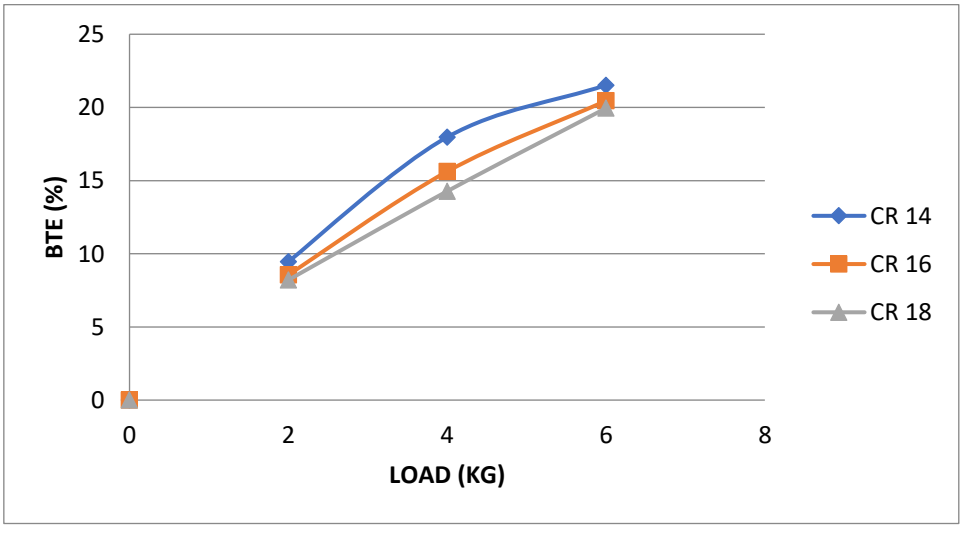

Fig 21. BTE variation of B10$Fe_2O_3$50 at CR 14, 16 and 18

Proceedings DOI: 10.21467/proceedings.7.6
ISBN: 978-81-989164-9-5

Series: AIJR Proceedings
ISSN: 2582-3922

Impact of CR on BTE. The BTE is observed to increase for the entire CR as shown in Fig 21 where the highest BTE is generated at CR 14 of B 10 Fe_2O_3 50. At compression ratio 18, Minimum BTE was obtained with value of 19.84%. Along with these, lower BFSC and better BP at compression ratio 14 also leads to higher BTE.

Table 3. BTE CR 14, 16, and 18 and full load

BTE (%) at conditions of full load			
Compression Ratio	14	16	18
D 100	19.44	19.25	18.76
B 10	19.12	18.71	18.9
B 10 $Fe_2O_3$50	20.41	19.35	18.84
B 15	18.34	18.04	17.39
B 15$Fe_2O_3$50	19.31	18.89	18.49

Fuel consumption (FC).

Impact of blend and load. The diesel and biodiesel blends were observed consumed fuel more experimentally with increase in load as illustrated in Fig 22, 23 and 24. B 10 Fe_2O_3 50 showed minimum FC amongst all the fuels as observed in Fig21.Table 4 gives the FC values observed at different load with CR 14,16, and 18.

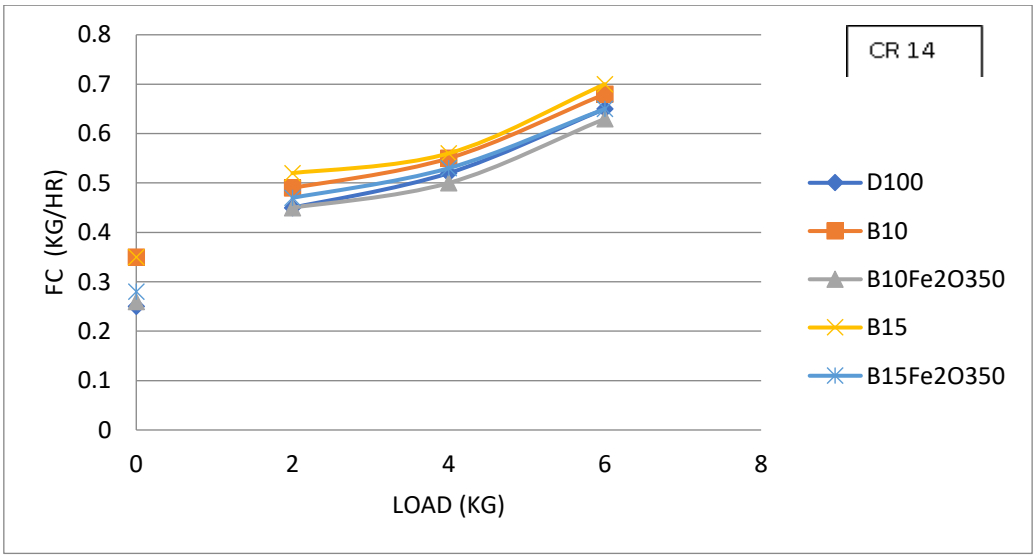

Fig.22. Fuel consumption at CR 14

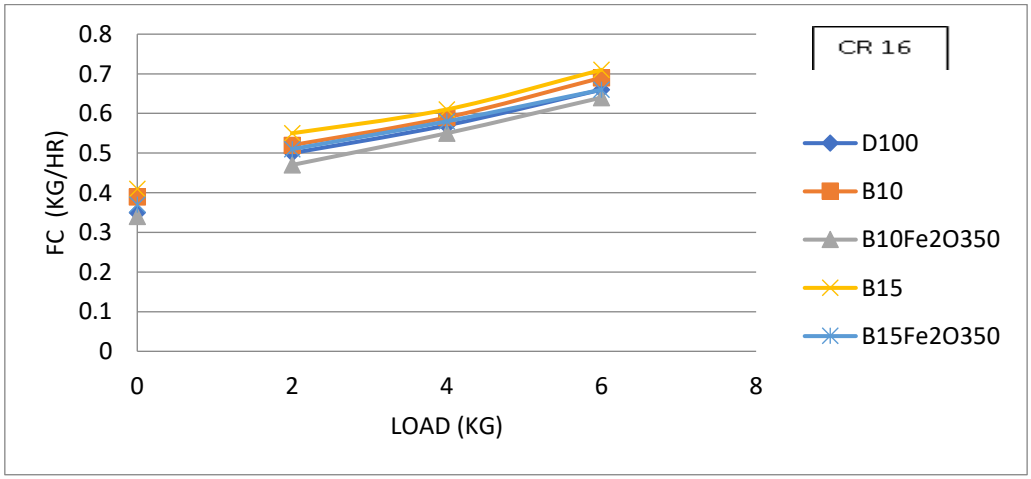

Fig.23. Fuel consumption at CR 16

Proceedings DOI: 10.21467/proceedings.7.6
ISBN: 978-81-989164-9-5

Series: AIJR Proceedings
ISSN: 2582-3922

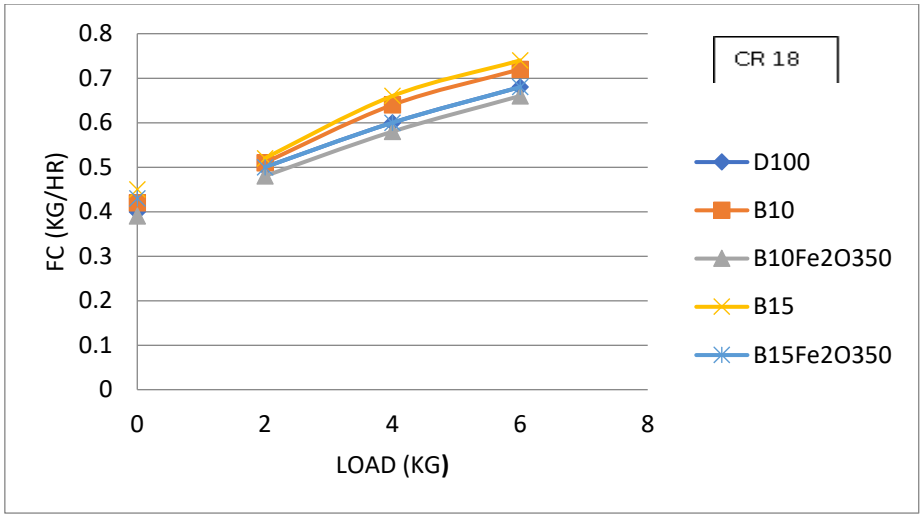

Fig.24. Fuel consumption at CR 18

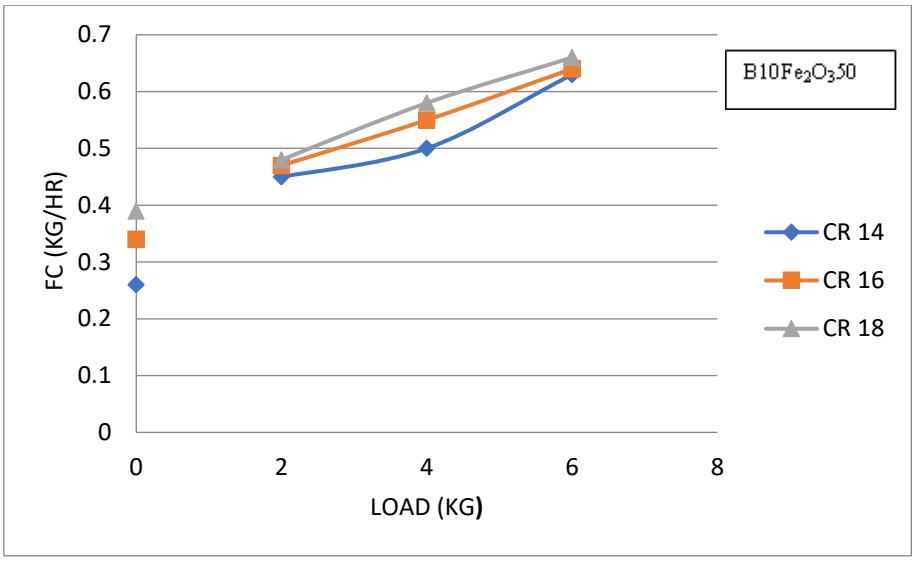

Fig.25. FC of B 10 Fe_2O_3 50 at CR 14, 16 and 18

Table 4. Fuel consumption variation

CR	LOAD	D 100	B 10	B 10 Fe_2O_3 50	B 15	B 15 Fe_2O_3 50
14	0	0.23	0.33	0.24	0.33	0.27
	2	0.43	0.47	0.43	0.51	0.46
	4	0.52	0.55	0.5	0.56	0.53
	6	0.65	0.68	0.63	0.7	0.65
16	0	0.35	0.39	0.34	0.41	0.37
	2	0.5	0.52	0.47	0.55	0.51
	4	0.57	0.59	0.55	0.61	0.58
	6	0.66	0.69	0.64	0.71	0.66
18	0	0.4	0.42	0.39	0.45	0.43
	2	0.5	0.51	0.48	0.52	0.5
	4	0.6	0.64	0.58	0.66	0.6
	6	0.68	0.72	0.66	0.74	0.68

Proceedings DOI: 10.21467/proceedings.7.6
ISBN: 978-81-989164-9-5

Series: AIJR Proceedings
ISSN: 2582-3922

Impact of CR on FC. The fuel was consumed more as the CR increased from 14 to 18. Amongst all the sample blends, B 10 Fe_2O_3 50 consumed the least fuel at all CR and full load. It was found to be the lowest at CR 14. Table 5 illustrates the variation in compression ratio of B 10 Fe_2O_3 50 blend at full load.

Table 5. Consumption of fuel with all load

FC (kg/hr) for full load			
Compression Ratio	14	16	18
D 100	0.64	0.65	0.67
B 10	0.67	0.68	0.71
B 10 Fe_2O_3 50	0.62	0.63	0.65
B 15	0.69	0.70	0.73
B 15 Fe_2O_3 50	0.64	0.65	0.67

BSFC.

Impact of blend and load on BSFC. The test was conducted for samples of diesel as well as the various samples of biodiesel blends B 10, B 10 $Fe_2O_3$50, B 15, B 15 Fe_2O_3 50 with load varying in the range 0-6 kg at CR 14, 16, and 18 as demonstrated in Fig 26, 27, and 28. The BFSC was observed to reduce steeply with load for all the samples taken at all compression ratio. The BFSC of blends of biodiesel sample B 15 and B 10 was experimentally elevated than the diesel and blend with nanoparticles . When 50ppm concentration nanoparticle added biodiesel sample was experimented on CI engine, the BFSC rose with the increase trend of biodiesel blend if compared to the neat diesel, B 10 and B 15. Additionally, lower BFSC was obtained for B 10 Fe_2O_3 50 characteristic to the higher CV in all the fuels, enhanced atomization and good combustion. Table 6 demonstrates the result obtained for all sample fuel blends at increased load with all CR.

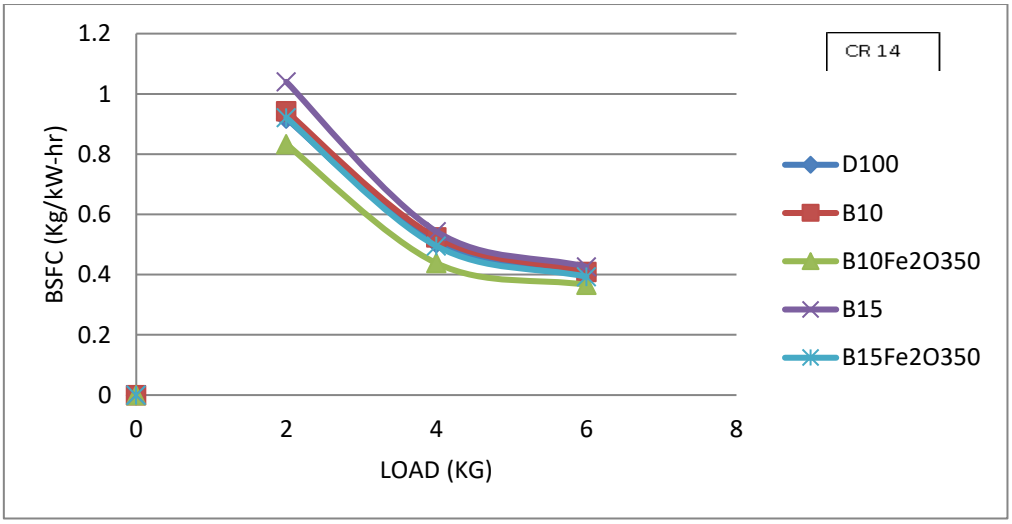

Fig.26. BSFC variation at CR 14

Proceedings DOI: 10.21467/proceedings.7.6
ISBN: 978-81-989164-9-5

Series: AIJR Proceedings
ISSN: 2582-3922

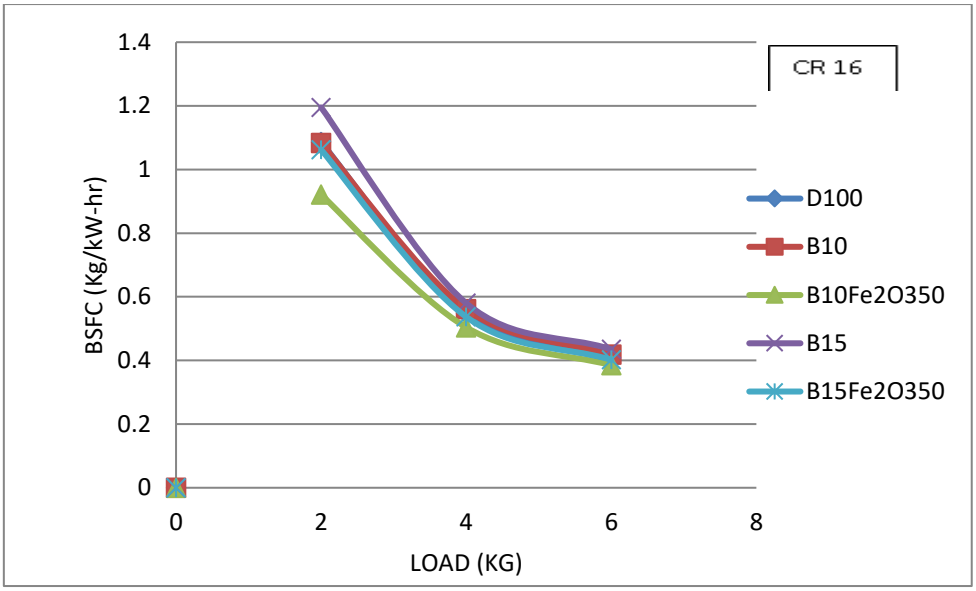

Fig.27. BSFC variation at CR 16

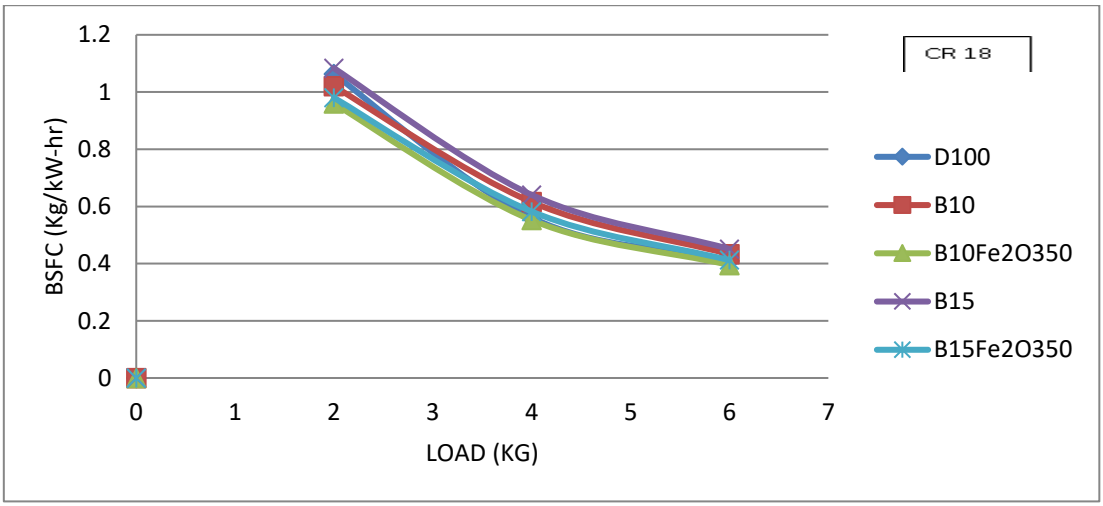

Fig.28. BSFC variation at CR 16

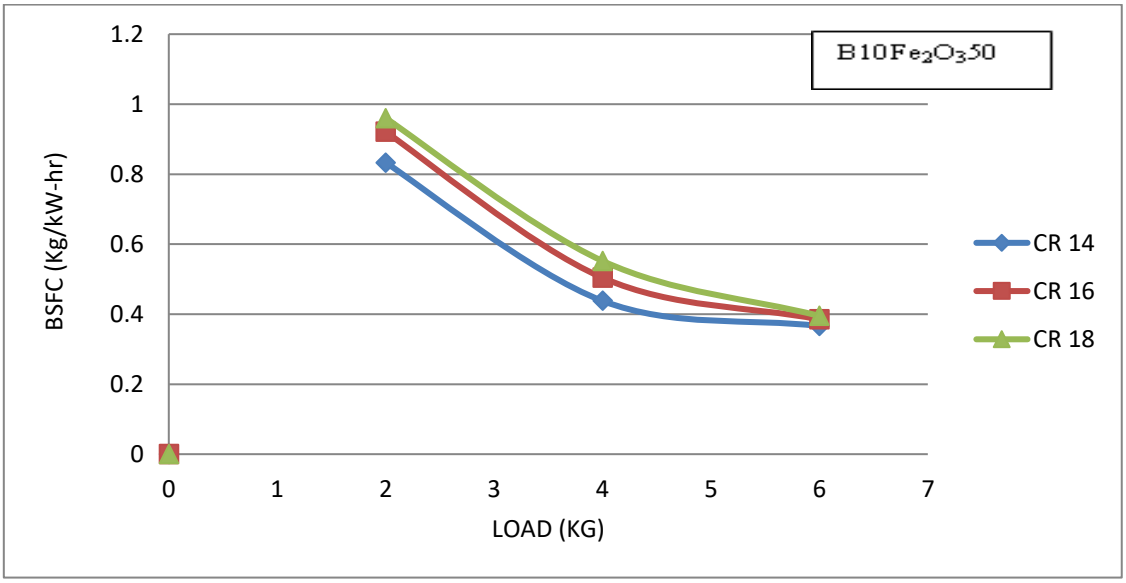

Fig.29. BSFC variation of B 10 Fe_2O_3 50 at CR 14,16, 18

Proceedings DOI: 10.21467/proceedings.7.6
ISBN: 978-81-989164-9-5

Series: AIJR Proceedings
ISSN: 2582-3922

Impact of CR on BSFC. The BFSC increased experimentally as the CR elevated in range 14 to 18. The BSFC at CR 14 was observed to be lesser than ones at CR 16 and CR 18. Among all the sample blends with entire load at all CR, BFSC of B 10 Fe_2O_3 50 was seen to be the lowest. Fig 29 illustrated the variation with rise in CR of B 10 Fe_2O_3 50 blend.

Table 6. BFSC observed for all fuels at full loads for all CR

Brake Specific Fuel Consumption (kg/kW-hr) with full load conditions			
CR	14	16	18
D 100	0.39	0.4	0.41
B 10	0.41	0.42	0.43
B 10 Fe_2O_3 50	0.37	0.38	0.39
B 15	0.43	0.43	0.45
B 15 Fe_2O_3 50	0.39	0.40	0.41

Exhaust gas temperature (EGT).

Impact of blend and load on EGT . With increasing load of 0 kg to 6 kg with different CR 14, 16 and 18 during the engine operation, the graph for base fuel taken as neat diesel and blends of biodiesel B 10, B 10 Fe_2O_3 50, B 15, and B 15 Fe_2O_3 50 were illustrated in Fig 30, 31 and 32. At full load, the EGT for different compression ratios were demonstrated in Table 7.

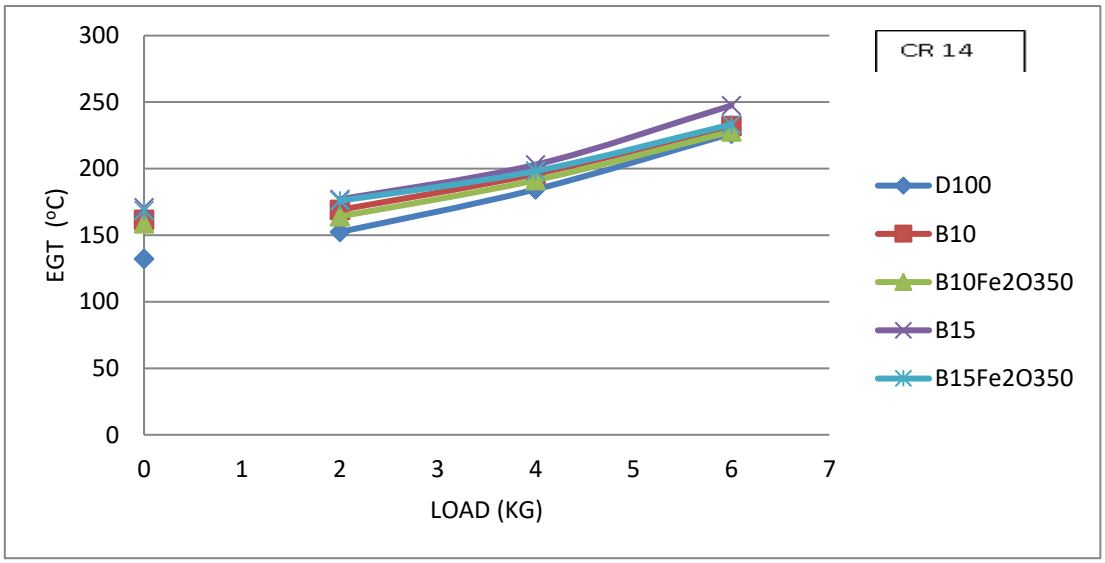

Fig.30. EGT variation at CR 14

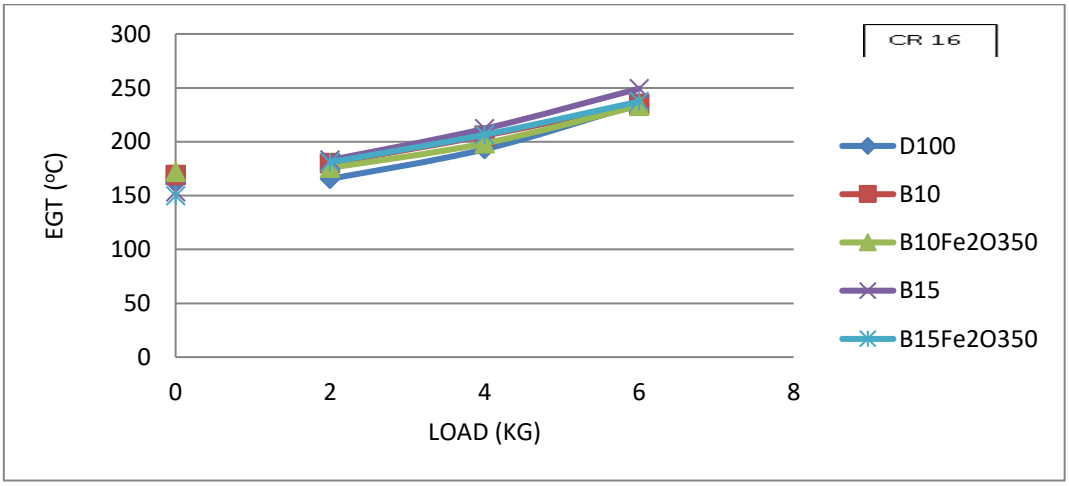

Fig.31. EGT variation at CR 16

Proceedings DOI: 10.21467/proceedings.7.6
ISBN: 978-81-989164-9-5

Series: AIJR Proceedings
ISSN: 2582-3922

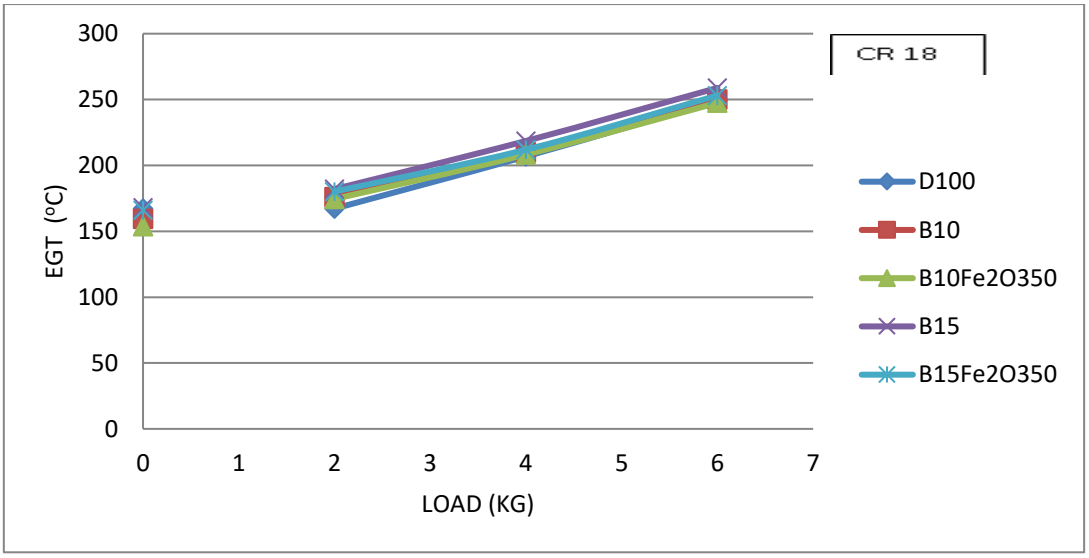

Fig.32. EGT variation at CR 18

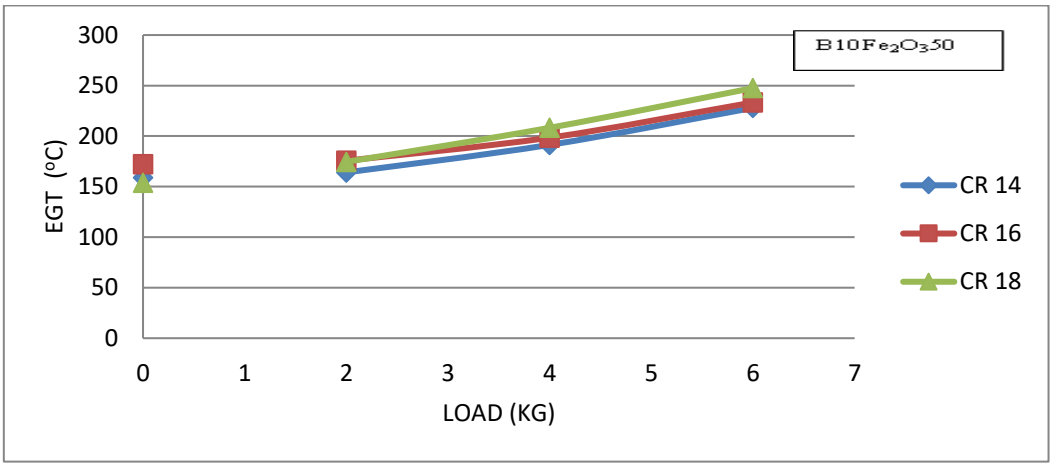

Fig.33. EGT variation of B 10 Fe_2O_3 50 at CR 14,16 and 18

Impact of CR on EGT. The EGT was increased when the CR increased from 14 to 18. The EGT was observed to reduce at CR 14 in contrast to CR 16 and 18. The EGT for B 10 Fe_2O_3 50 blend observed at 227.93°C, was higher than D 100 sample with complete load and CR 14. Moreover, B10 Fe_2O_3 50 blend had the least temperature in all the fuels including diesel for complete load and CR 16 and 18. These temperatures obtained were 233.31°C and 247.52 °C. The variations with rise in CR of B 10 Fe_2O_3 50 blend is shown in Fig33.

Table 7. Exhaust Gas Temperature

CR	LOAD	D 100	B 10	B 10 Fe_2O_3 50	B 15	B 15 Fe_2O_3 50
14	0kg	118.926	146.277	143.1	153.64	151.61
	2kg	137.19	152.145	147.69	159.34	158.32
	4kg	184.43	196.06	191.32	203	198.24
	6kg	226.38	231.93	227.93	247.5	233.24
16	0kg	164.1	169.16	172.12	153.34	149.56
	2kg	165.5	180	175.75	183	181
	4kg	192.99	205.59	198.46	212.05	206.46
	6kg	234.91	235.01	233.31	249.25	237.27
18	0kg	167.08	159.48	153.83	168.02	166
	2kg	167.19	175.89	174.52	182.02	180.17
	4kg	206.83	210.07	208.25	218.57	211.95
	6kg	249.09	250	247.52	258.85	253.07

Proceedings DOI: 10.21467/proceedings.7.6
ISBN: 978-81-989164-9-5

Series: AIJR Proceedings
ISSN: 2582-3922

4.3 Emission Characteristics

NOx

Impact of blend and load on NO_X emission. The varied values of NOx emission for different samples of blends of biodiesel in regards of load at CR 14, 16 and 18 are illustrated in Fig 34, 35 and 36. The outcomes obtained of NOx are demonstrated in Table 8.

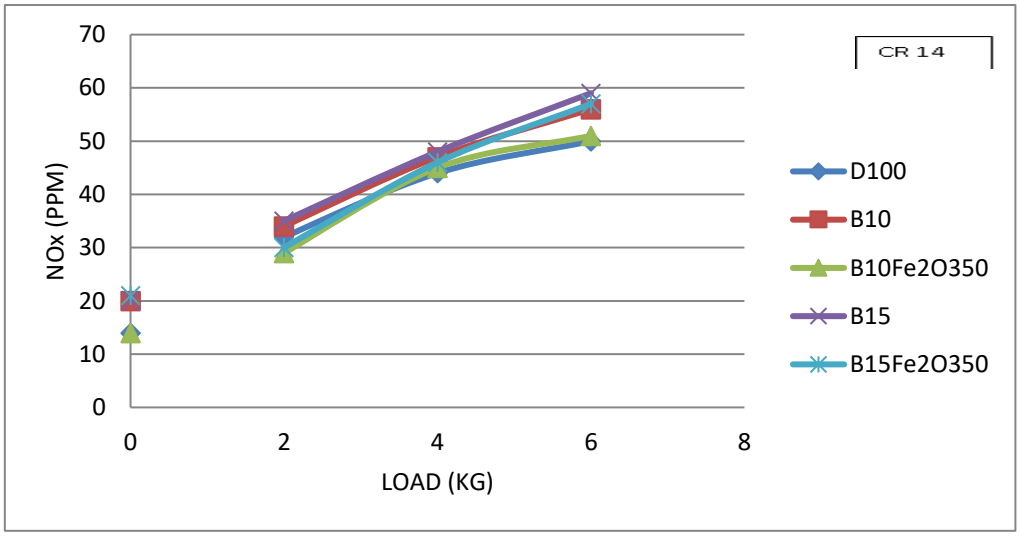

Fig.34. NOx variation at CR 14

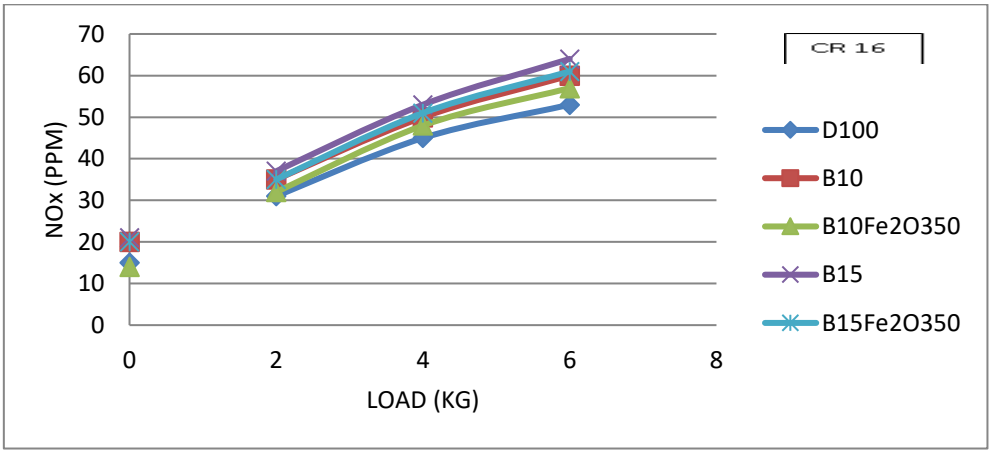

Fig.35. NOx variation at CR 16

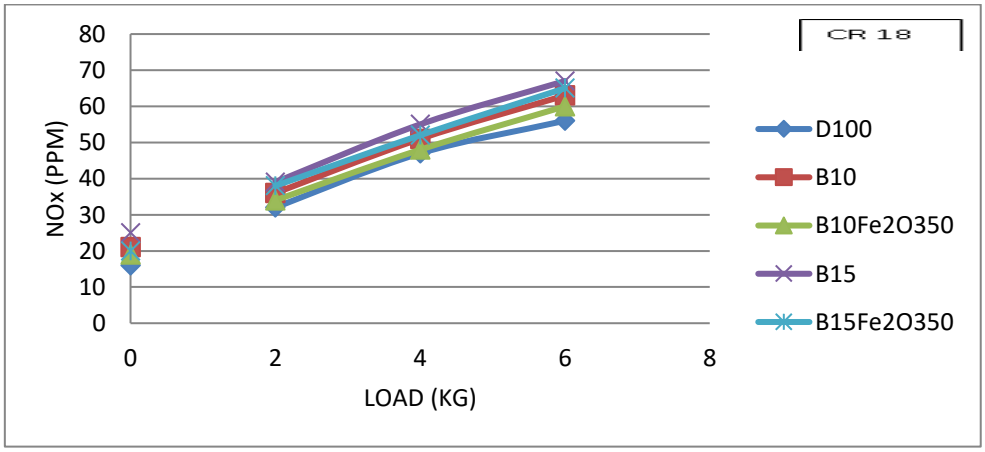

Fig.36. NOx variation at CR 18

Proceedings DOI: 10.21467/proceedings.7.6
ISBN: 978-81-989164-9-5

Series: AIJR Proceedings
ISSN: 2582-3922

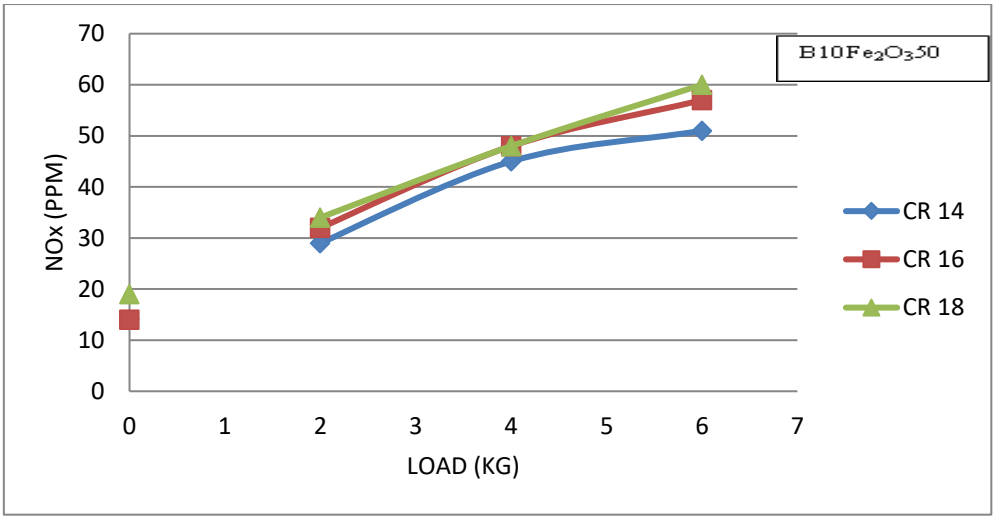

Fig.37. NO_X variation of B10Fe2O350 at CR 14, 16, and 18

Impact of CR on NO_X emission. The NO_X emissions was increased experimentally with the rise in CR from 14 to 18. The blend B 10 Fe_2O_3 50 was seen to be optimized for CR 14 and could be depicted clearly from Fig37. The B 10 Fe_2O_3 50 blend was found to be 8.92% reduced NO_X with maximum load in contrast with B10. It nearly showed the same values as that of neat diesel for all loads and CRs. Fig 37 clearly shows the NO_X emissions varying as the CR of B 10 Fe_2O_3 50 blend increases.

Table 8. NO_X results at various loads and CR (ppm)

CR	LOAD	D 100	B 10	B 10 Fe_2O_3 50	B 15	B15 Fe_2O_3 50
14	0	7	10	7	10	11
	2	16	17	15	18	15
	4	42	45	43	46	44
	6	48	54	49	57	55
16	0	13	18	12	19	18
	2	29	33	30	35	33
	4	45	50	48	53	51
	6	53	60	57	64	61
18	0	16	21	19	25	20
	2	32	36	34	39	38
	4	47	51	48	55	52
	6	56	63	60	67	65

CO.

Impact of blend and load on CO emission . The CO emission varies for pure diesel fuel and various biodiesel blends B 10, B 10 Fe_2O_3 50, B 15, and B15 $Fe_2O_3$50 for varying value of compression ratio ranging from 14 to 18 and is depicted in Fig 38, 39, and 40. The pure diesel showed the maximum emission of CO when compared to other fuels. Moreover, biodiesel blends B10 and B15 showed improvement and reduced CO emissions in contrast with pure diesel. The dispersion of iron oxide nanoparticles resulted in further improvement. At each load and CR, the minimum carbon monoxide was emitted by B 15 Fe_2O_3 50 biodiesel blend. The results obtained are illustrated for complete load and CR 14, 16 and 18 in Table 9.

Proceedings DOI: 10.21467/proceedings.7.6
ISBN: 978-81-989164-9-5

Series: AIJR Proceedings
ISSN: 2582-3922

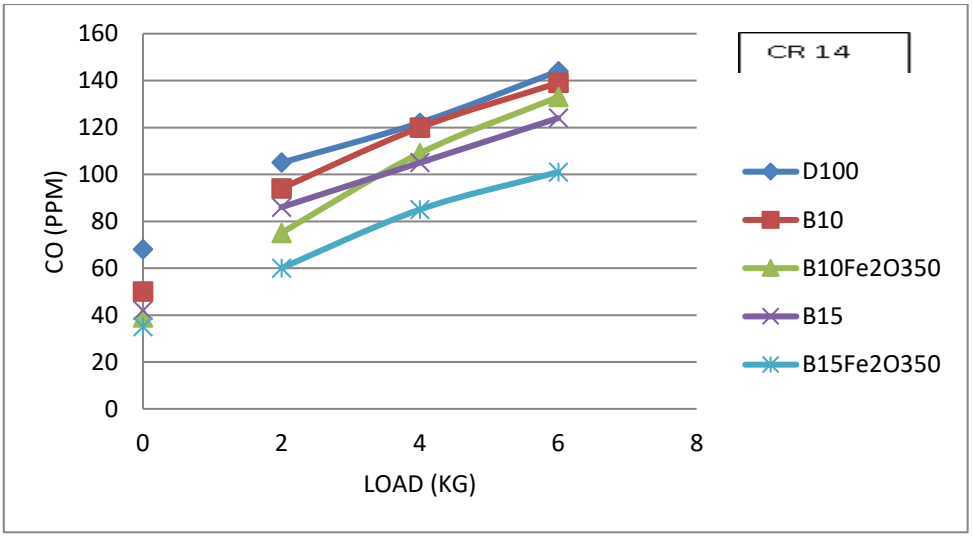

Fig.38. CO variation at CR 14

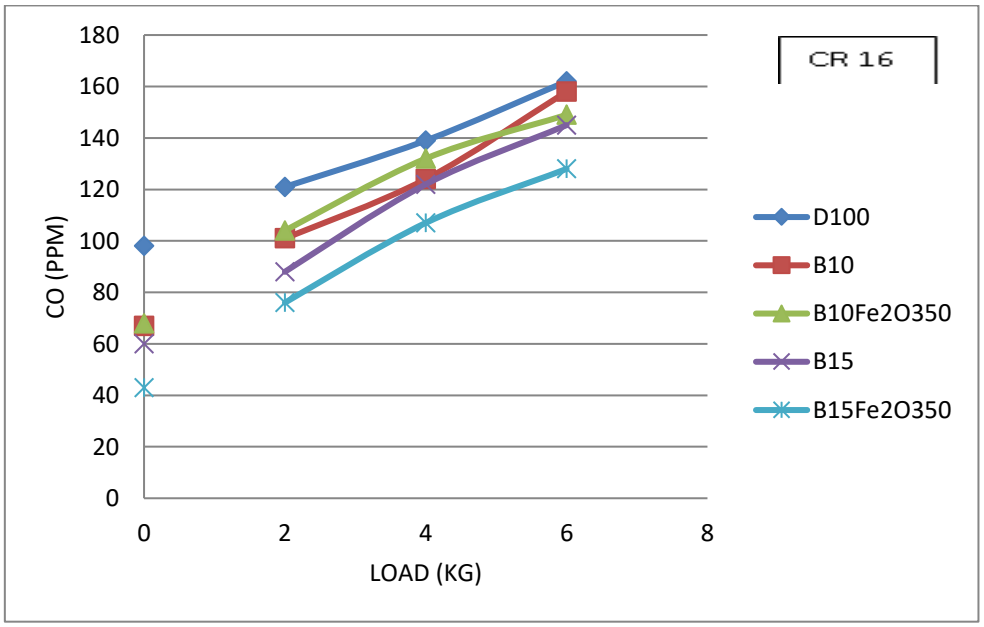

Fig.39. CO variation at CR 16

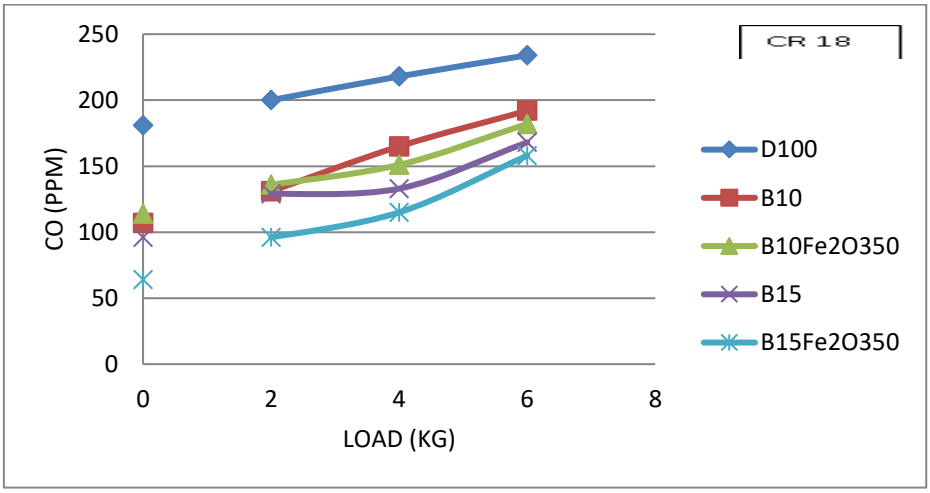

Fig.40. CO variation at CR 18

Proceedings DOI: 10.21467/proceedings.7.6
ISBN: 978-81-989164-9-5

Series: AIJR Proceedings
ISSN: 2582-3922

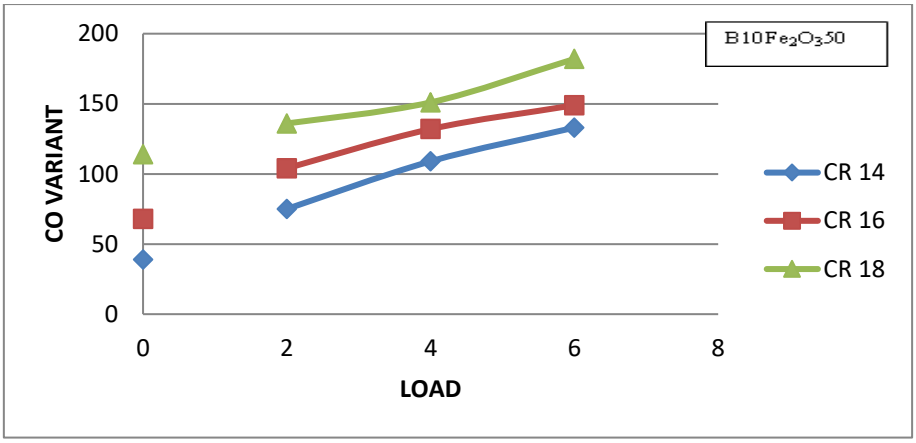

Fig.41. CO variation of B15Fe2O350 at CR 14, 16, and 18

Impact of CR on CO emission. The CO at CR 14 was found to be lesser than that of compression ratios 16 and 18. However, the B 15 Fe_2O_3 blend was experimentally the lowest within all the fuel blends at each load and CR. The result obtained of CO emission of B 15 Fe_2O_3 is demonstrated in Fig 41.

Table 9. CO results of each fuel sample at various loads and CR (ppm)

CR	LOAD	D 100	B 10	B 10 Fe_2O_3 50	B 15	B 15 Fe_2O_3 50
14	0	34	25	20	21	18
	2	53	47	38	43	30
	4	122	120	109	105	85
	6	144	139	133	124	101
16	0	98	67	68	60	43
	2	121	101	104	88	76
	4	139	124	132	122	107
	6	162	158	149	145	128
18	0	181	107	114	96	64
	2	200	131	136	129	96
	4	218	165	151	133	115
	6	234	192	182	168	158

HC.

Impact of blend and load on HC emission. The HC emission varies with load for pure diesel as well as sample blends B 10, B 10 Fe_2O_3 50, B 15 and B15$Fe_2O_3$50 at CR 14, 16 and 18 which is demonstrated in Fig 42, 43 and 44. The hydrocarbon produced was found experimentally to be the least for diesel, B 10 Fe_2O_3 50 and B 15 Fe_2O_3 50, with the others fuels emitting it within permissible limits. The hydrocarbons exhibited by B 10 and B 15 were at higher amount for no load and CR 14, 16 and 18.

Proceedings DOI: 10.21467/proceedings.7.6
ISBN: 978-81-989164-9-5

Series: AIJR Proceedings
ISSN: 2582-3922

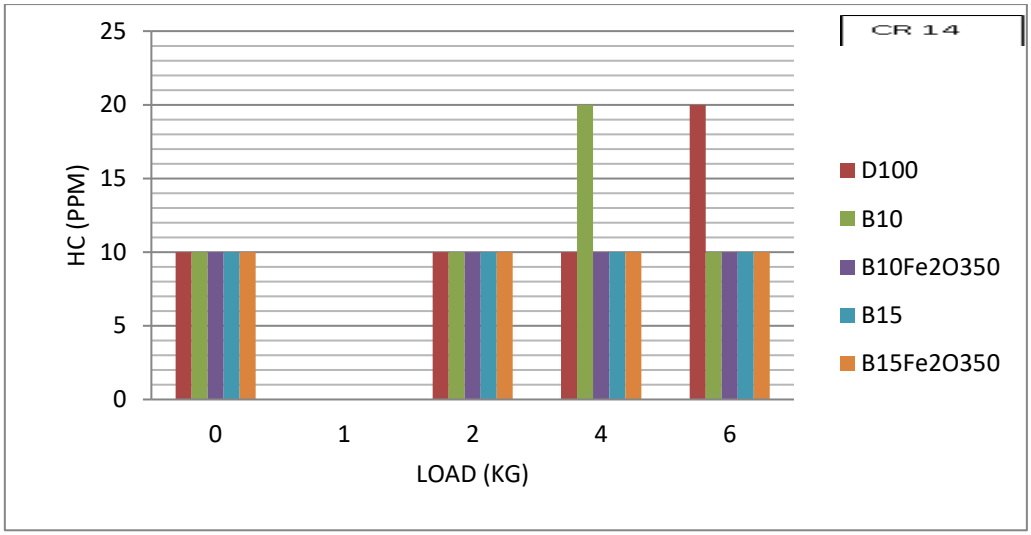

Fig.42. HC variation at CR 14

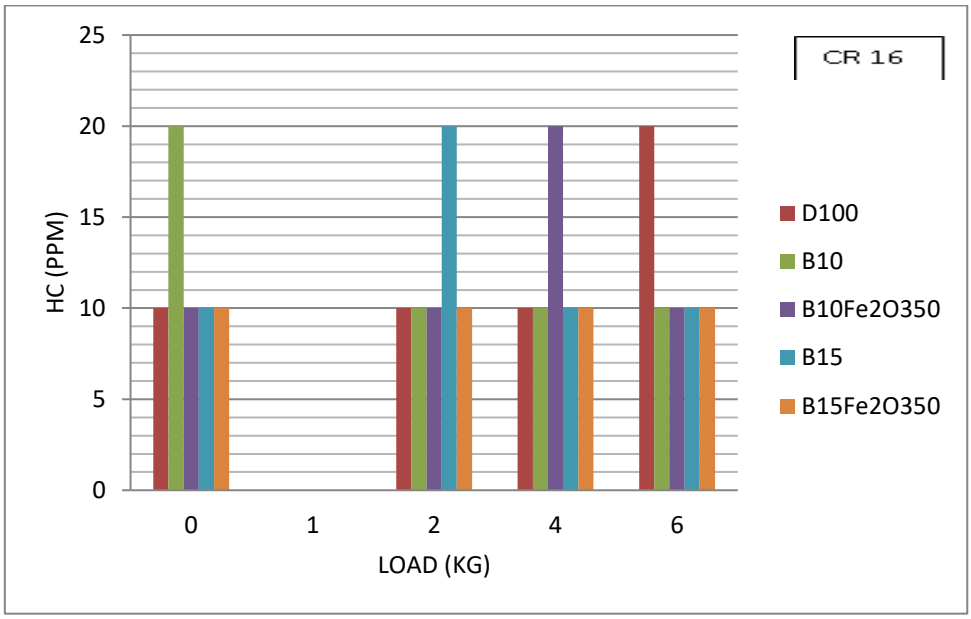

Fig.43. HC variation at CR16

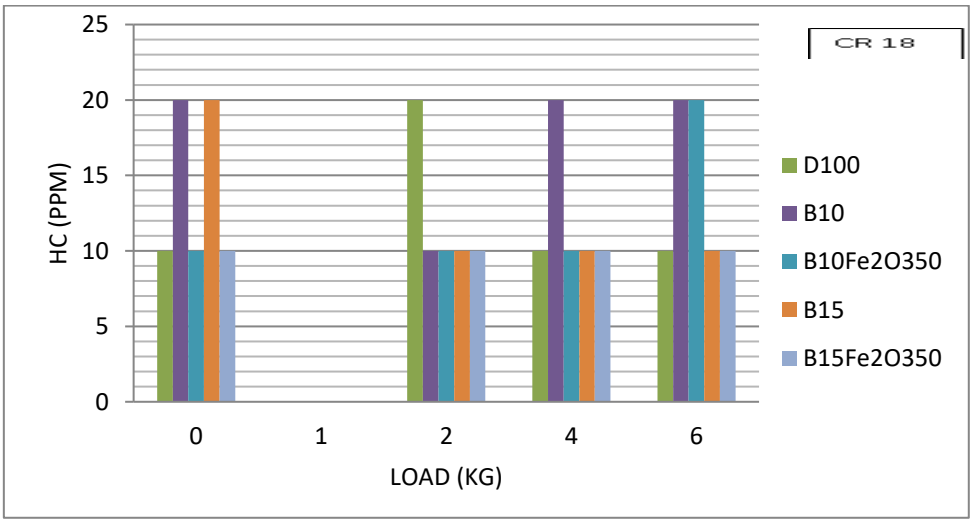

Fig.44. HC variation at CR 18

Proceedings DOI: 10.21467/proceedings.7.6
ISBN: 978-81-989164-9-5

Series: AIJR Proceedings
ISSN: 2582-3922

Table 10. HC results at various loads and CR

CR	LOAD (KG)	D 100	B 10	B 10 Fe_2O_3 50	B 15	B 15 Fe_2O_3 50
14	0	9	7	8	9	9
	2	8	9	7	9	10
	4	10	20	10	10	10
	6	20	10	10	10	10
16	0	10	20	10	10	10
	2	10	10	10	20	10
	4	10	10	20	10	10
	6	20	10	10	10	10
18	0	10	20	10	20	10
	2	20	10	10	10	10
	4	10	20	10	10	10
	6	10	20	20	10	10

X Ray Diffraction

The X Ray Diffraction was used to confirm the formation of γ-Fe_2O_3 nanoparticles and the XRD plots of γ-Fe_2O_3 are demonstrated in Fig 45. In accordance with the standard XRD pattern of γ-Fe2O3 Powder Diffraction File, JCPDS No. 39-1346, the primary peaks of γ-Fe2O3 were found at 2θ = 30.28, 35.68, 43.34, 53.80, 57.34, and 62.95°. These reflections correspond to the (110), (155), (200), (211), (255), and (220). The Scherer's formula is being utilized in line broadening to evaluate the crystallite size of the γ-Fe_2O_3 nanoparticles as shown in equation (1).

$$D = \frac{k\lambda}{\beta} cos\theta \quad ..(1)$$

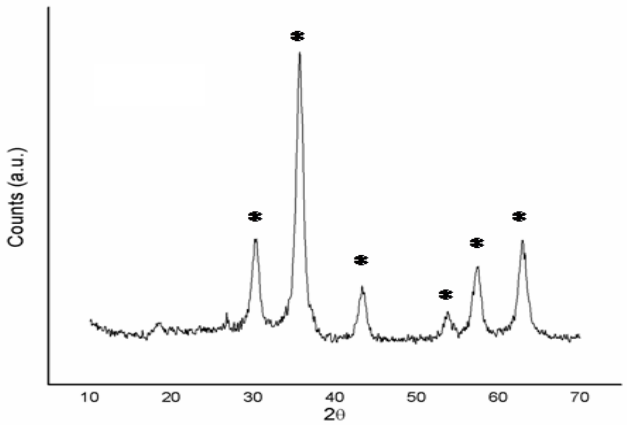

Fig.45. XRD

5. Conclusion

The conventional fuels once considered as major energy resources are non-renewable in nature and could be depleted exponentially with the rise in demand. Additionally excess use of these sources is detrimental to the living and surroundings. This called for the need for greener and more accessible energy source to be used instead of fossil fuels. The study was aimed to investigate the waste cooking oil as a promising alternative to be used as biofuel with the dispersion of iron oxide nanoparticles to enhance its properties. The cooking oil often disregarded as waste oil is in abundant quantity in India making it feasible and accessible as a fuel resource. A comparative analysis was achieved experimentally among the neat diesel fuel, biodiesel blends with and without nanoparticles to determine the various fuel and emission characteristics, performance when tested in a variable CI engine. The biodiesel manufacturing process's response attributes in relation to the process parameters are determined as well via machine learning models, specifically linear regression and random forest regression. According to the investigation, the linear regression approach can only reach modest accuracy in biodiesel yield prediction modelling, while random forest regression exhibits very high accuracy. The biodiesel blends, without or with the addition of nanoparticles, were experimented to determine the optimal configuration of the blend for improved efficacy and reduced emissions. These

Proceedings DOI: 10.21467/proceedings.7.6
ISBN: 978-81-989164-9-5

Series: AIJR Proceedings
ISSN: 2582-3922

nanoparticles were observed to enhance the overall characteristics of the fuel. The biodiesel blend B10$Fe_2O_3$50, comprising of 50ppm concentration of iron oxide nanoparticles showed promising results at compression ratio 14 amongst all the fuels. Moreover, this blend was characterized experimentally with the highest brake thermal efficiency, outperforming pure diesel and its own blend without the nanoparticles, B10 with improvement of 4.72% and 6.37% respectively. As the solution needs to be cleaner due to the degradable state of current environment, the various emission exhibitions were also analysed. B10$Fe_2O_3$50 showed signification reductions in the terms of emissions. It observed a decrease in NO_X emission up to 8.92%lower than B10, CO emissions which were 7.63% lower than neat diesel, and maintained HC emissions within permissible limits. These results demonstrated B10$Fe_2O_3$50 as the efficient, accessible and environmentally favourable biodiesel blend. Further, glycerol, a side product obtained during the biodiesel production could be leveraged as a potential lubricant in industrial applications. This eliminates the potential wastage of the by-products obtained in the process. Moving ahead, more work is to be done to explore the wider range of nanoparticles having different sized and materials with fuels along with the analysis of the stability of fuel for long periods using surfactants. Optimization of agitation speed and sonication time is required as well. There is also the need for prolonged operation of the engine, including the evaluation of exhaust emission containing nanoparticles, and additional experimentation on engine parameters like angular shaft rotation speed, injection timing and delay before ignition. Evaluation of frictional characteristics of nano fuels is essential, along with the design and implementation of sound control policies. Economical assessment of the feasibility for mass production of those nano fuel biodiesel technologies will be necessary too.

References

[1] M. V. Rodionova, R. S. Poudyal, I. Tiwari, R. A. Voloshin, S. K. Zharmukhamedov, H. G. Nam, B. K. Zayadan, B. D. Bruce, H. J. M. Hou, and S. I. Allakhverdiev, "Biofuel production: Challenges and opportunities," *International Journal of Hydrogen Energy*, vol. 42, no. 12, pp. 8450–8461, 2017, doi: 10.1016/j.ijhydene.2016.11.125.

[2] A. C. Pinto, L. L. N. Guarieiro, M. J. C. Rezende, N. M. Ribeiro, E. A. Torres, W. A. Lopes, P. A. de P. Pereira, and J. B. de Andrade, "Biodiesel: An overview," *Journal of the Brazilian Chemical Society*, vol. 16, no. 6B, pp. 1313–1330, 2005, doi: 10.1590/S0103-50532005000800003..

[3] P. T. Vasudevan and M. Briggs, "Biodiesel production—current state of the art and challenges," *Journal of Industrial Microbiology & Biotechnology*, vol. 35, pp. 421–430, 2008, doi: 10.1007/s10295-008-0312-2.

[4] F. Cherubini and A. H. Strømman, "Life cycle assessment of bioenergy systems: State of the art and future challenges," *Bioresource Technology*, vol. 102, no. 2, pp. 437–451, 2011, doi: 10.1016/j.biortech.2010.08.010

[5] J. L. Parcell and P. Westhoff, "Economic effects of biofuel production on states and rural communities," *Journal of Agricultural and Applied Economics*, vol. 38, no. 2, pp. 377–387, 2006, doi: 10.1017/S1074070800022353

[6] P. Murali, K. Hari, and D. P. Prathap, "An economic analysis of biofuel production and food security in India," *Sugar Tech*, vol. 18, no. 5, pp. 449–456, 2016, doi: 10.1007/s12355-015-0412-z

[7] S. A. Kadapure, P. Kirti, S. Singh, S. Kokatnur, N. Hiremath, A. Variar, S. Shaikh, and R. Chittaragi, "Studies on process optimization of biodiesel production from waste cooking and palm oil," *Biofuels*, vol. 9, no. 5, pp. 631–641, 2017, doi: 10.1080/19397038.2017.1420107.

[8] M. Balaji and M. Cheralathan, "Experimental investigation of a DI diesel engine fueled with neat biodiesel and biodiesel-metal oxide nanoparticle blends," *International Journal of Green Energy*, vol. 12, no. 6, pp. 542–548, 2015, doi: 10.1080/15435075.2013.875071.

[9] S. Mahalingam, T. Sundararajan, and S. Ramanathan, "An investigation on the effect of Fe_3O_4 nanoparticles as additive with biodiesel in CI engine," *International Journal of Ambient Energy*, vol. 39, no. 4, pp. 398–404, 2018, doi: 10.1080/01430750.2017.1307642.

[10] M. P. Sudeshkumar and G. Devaradjane, "Experimental analysis on the blends of oxygenated fuels with diesel in a direct injection diesel engine for performance evaluation and emissions," *Materials Science Research India*, vol. 7, no. 1, 2010, doi: 10.13005/msri/070130

[11] R. Sarin, M. Sharma, S. Sinharay, and R. K. Malhotra, "Jatropha–Palm biodiesel blends: An optimum mix for Asia," *Fuel*, vol. 86, no. 10–11, pp. 1365–1371, 2007, doi: 10.1016/j.fuel.2006.11.040

[12] M. K. Baig, M. S. Mirza, T. Parveen, and S. Ilyas, "Enhancing performance of biodiesel blends with aluminum oxide nanoparticles through ultrasonication," *Discover Energy*, vol. 2, no. 1, pp. 1–12, 2022, doi: 10.1186/s44147-022-00127-y.

[13] B. Sajjadi, A. A. A. Raman, and H. Arandiyan, "A comprehensive review on properties of edible and non-edible vegetable oil-based biodiesel: Composition, production, stability, and performance," *Renewable and Sustainable Energy Reviews*, vol. 63, pp. 62–92, 2016, doi: 10.1016/j.rser.2016.05.050.

[14] S. Gautam, S. Kanakraj, and A. Henry, "Computational approach using machine learning modelling for optimization of transesterification process for linseed biodiesel production," *AIMS Bioengineering*, vol. 9, no. 4, pp. 319–336, 2022, doi: 10.3934/bioeng.2022023.

[15] K. K. Gupta, K. Kalita, R. K. Ghadai, M. Ramachandran, and X.-Z. Gao, "Machine learning-based predictive modelling of biodiesel production—A comparative perspective," *Energies*, vol. 14, no. 4, p. 1122, 2021, doi: 10.3390/en14041122.

[16] M. Sonachalam, V. Manieniyan, R. Senthilkumar, R. MK, M. Warimani, R. Kumar, A. Kedia, T. Y. Khan, and N. Almakayeel, "Experimental investigation of performance, emission, and combustion characteristics of a diesel engine using blends of waste cooking oil-ethanol biodiesel with MWCNT nanoparticles," *Case Studies in Thermal Engineering*, vol. 61, p. 105094, 2024, doi: 10.1016/j.csite.2024.105094.

[17] A. Sharma, M. Kumar, and S. Singh, "Determination and analysis of flash point and fire point of biofuels for combustion applications," *Fire Technology*, vol. 59, pp. 1923–1938, 2023, doi: 10.1007/s10694-023-01449-w.